VALIDATION OF IMPINGING JET MODELS TO BE USED IN CANDU CALANDRIA VESSEL CFD SIMULATIONS

M. Bouquillon[1], A. Teyssedou*[1], E. Cuesta[1] & H. Huynh[2]

[1] Nuclear Engineering Institute, Engineering Physics Department
École Polytechnique de Montréal
CANADA

[2] Hydro-Québec, Montréal
CANADA

ABSTRACT

The knowledge of the external wall temperature distributions on calandria tubes is of major concern in nuclear safety analysis. Therefore, a full-scale modeling of the moderator using Computational Fluid Dynamic models is necessary. The use of a 2D CFD model have shown that the geometry of calandria nozzles has a strong effect on the flow distribution. However, obtaining realistic data about inlet conditions constitutes a difficult task because of the complexity of the turbulent jet dynamics as well as the strong difference of the mesh characteristic length between the nozzles and the calandria vessel. Therefore, the present study is aimed to find appropriate water-jet modeling approaches that can help us in improving moderator circulation simulations. The principal interest consists of finding a semi-analytical nozzle model that can be used as a constitutive relationship in a CFD code. This approach will contribute both to increase the number of meshes in the calandria vessel as well as to decrease the computational time.

1. INTRODUCTION

The knowledge of the external wall temperature distributions on calandria tubes is of major concern in nuclear safety analysis. Some experimental simulations of the moderator circulation were carried out using scaled-down set-ups (Hadaller et al. [1]). Analytical models were developed by replacing the calandria by an equivalent porous media with appropriate anisotropic hydraulic resistances (Huget et al. [2]; Yoon et al. [3]). This technique has the advantage of treating a non-connected domain as an equivalent quasi-continuous media. Some efforts have been also deployed to validate this type of modeling approach (Huget et al. [2]; Carlucci et al. [4]). However, this type of calculations cannot provide information about local velocity variations.

Within the framework of the present study, a full-scale modeling of the moderator using a Computational Fluid Dynamic code (FLUENT) is underway. A previous use of a 2D model has shown that the geometry of calandria nozzles has a strong effect on the flow distribution. Yoon & Park [5] suggested to model the flow at the entrance of the calandria as successive flow circulations through a portion of a straight pipe, a curved pipe, and a circular nozzle placed in front of an impinging plate, and to use the results as input data in full-scale calculations. Obtaining these data requires large computational resources before performing complete flow simulations, while they do necessarily represent neither the real geometry nor the actual flow conditions. The aim of the present work consists of finding a semi-analytical nozzle model that can be used as a constitutive relationship in a CFD code. To this purpose, a CFD jet model is validated to generate the required data for ulterior development of an appropriate nozzle correlation. This approach will contribute both to increase the number of meshes in the calandria vessel as well as to decrease the computational time.

2. TURBULENT FLOW EQUATIONS

The κ-ω SST turbulent model is used for carrying out the numerical simulations, which instead of using an instantaneous formulation; it uses Reynolds-Averaged Navier-Stokes (RANS) equations. These equations are summarized as:

* Corresponding author: alberto.teyssedou@polymtl.ca

$$\frac{\partial \rho}{\partial t} + \vec{\nabla}\left(\rho \vec{u}\right) = 0 \tag{1}$$

$$\frac{\partial\left(\rho \vec{u}\right)}{\partial t} + \vec{\nabla}.\left(\rho \vec{u} \otimes \vec{u}\right) = -\vec{\nabla} p + \mu \nabla^2 \vec{u} + \rho \vec{g} + \text{Reynolds Stresses} \tag{2}$$

It is apparent that to solve this system two additional equations are required. The new equations satisfy the transport of turbulent kinetic energy κ and its dissipations rate ω; they are written as:

$$\frac{\partial}{\partial t}(\rho k) + \frac{\partial}{\partial x_i}(\rho k u_i) = \frac{\partial}{\partial x_j}\left(\Gamma_k \frac{\partial k}{\partial x_j}\right) + \tilde{G}_k - Y_k + S_k \,, \tag{3}$$

$$\frac{\partial}{\partial t}(\rho \omega) + \frac{\partial}{\partial x_i}(\rho \omega u_i) = \frac{\partial}{\partial x_j}\left(\Gamma_\omega \frac{\partial \omega}{\partial x_j}\right) + G_\omega - Y_\omega + D_\omega + S_\omega \,, \tag{4}$$

The κ-ω SST model is in close agreement with measurements of plane and round jets which spread over one or several walls. It also permits to combine the accurate approach of the κ-ω equations in the near-wall region with the most popular κ-ε solver for simulating far flow field zones. More details about the coefficients included in these equations are given in [6].

3. FLOW MODELING SCHEME AND BOUNDARY CONDITIONS

Due to the geometry of the jet, the domain can be reduced to an axis-symmetric bi-dimensional problem. The jet inlet velocity is characterized by a time-averaged fully developed turbulent profile and a given turbulent intensity. Atmospheric pressure was applied at the exit as well as at the top of the domain (see Figure 1).

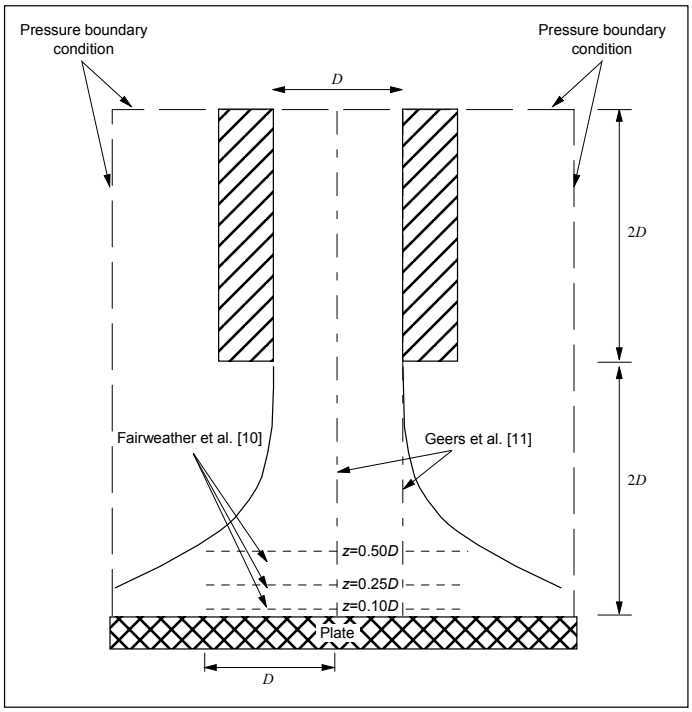

Figure 1. Geometrical scheme used to carry out FLUENT simulations.

The upper boundary condition permits to model secondary flows caused by the mean jet stream (i.e., the jet mass flow rate increases due to the secondary flow). Finer mesh was applied in the lower

part of the domain to capture all the wall boundary layer features and the enhanced wall treatment was used. More details about this approach are available on the FLUENT code user guide [6]. Figure 1 also shows the geometry used for the simulations and the locations where the numerical results where sampled for comparing with experimental data.

FLUENT uses a Non-Staggered Control Volume Storage Scheme (Ramezanpour et al. [7]); thus, it evaluates the flow properties at the center of each cell, which are then extrapolated using a pressure discretization scheme. The PRESTO! option is used because it is particularly adapted to strongly curved flows (Ramezanpour et al. [7]). The pressure based solver and the pressure-velocity coupling algorithm (SIMPLE) are used due to their robustness in treating incompressible flow problems.

4. COMPARISON OF FLUENT SIMULATIONS WITH EXPERIMENTAL DATA

The heat transfer from calandria tubes to the moderator depends on flow velocity distributions close to the tube walls as well as on the effect of turbulence close to stagnant regions. Therefore, these two features must be correctly modeled, in particular for moderator injection regions. Even though the mean flow characteristics can be easily calculated, modelling the effect of turbulence is always cumbersome. The major difficulty arises from the fact that most turbulent models tend to overestimate the turbulent kinetic energy. As it has been discussed before, the main objective of this work consists of establishing the best strategy for simulating impinging jets. To this aim, the results of the simulations are compared with the experimental data given in the open literature. Table 1 summarizes the principal characteristics of the experiments selected for the present work. With the exception of the results obtained from numerical simulations given in Hadžiabdić & Hanjalić [8], the rest of the referred research works contains experimental data. Note that these data have been collected using different measurement techniques. Moreover, two separate comparisons are presented; first the mean flow velocities calculated at different axial and radial locations are compared with available data, then the effect of turbulence on the simulations is discussed in detail.

Table 1. Summary of works used for validating the present simulations.

Reference	Inside Diameter (*mm*)	Wall Thickness δ/D	Discharge Distance z/D	Reynolds Number	Fluid	Type of Measurements
Cooper et al. [9]	101.6 26.0	0.0313	2	70000 23000	Air	Axial and radial (Hot-wire anemometer)
Faiweather & Hargrave [10]	13.3	NA	2	18800	Air	Radial (PIV)
Geers et al. [11]	36.0	NA	2	23000	Air	Axial r/D=0, r/D=0.5 (LDA and PIV)
Brison & Brun [12]	26.0	0.112	2	23000	Air	Axial r/D=0.5 (LDA and hot-wire anemometer)
Hadžiabdić & Hanjalić [8]	NA	NA	2	20000	NA	Simulations H/D=0.0125, H/D=0.05

NA: not available.

4.1 COMPARISON OF SIMULATED MEAN FLOW VELOCITIES WITH DATA

Yoon & Park [5] represented the moderator injection system in the calandria vessel of a CANDU-6 as an impinging jet. Their simulations were validated by using data given in Cooper et al. [9]. Herewith, the same experiments are simulated using the FLUENT code (see Figure 2). In general, the mean flow velocities at different radial locations calculated with FLUENT are in very good agreement with the data. At the flow centerline, however, the code underpredicts the experimental trends.

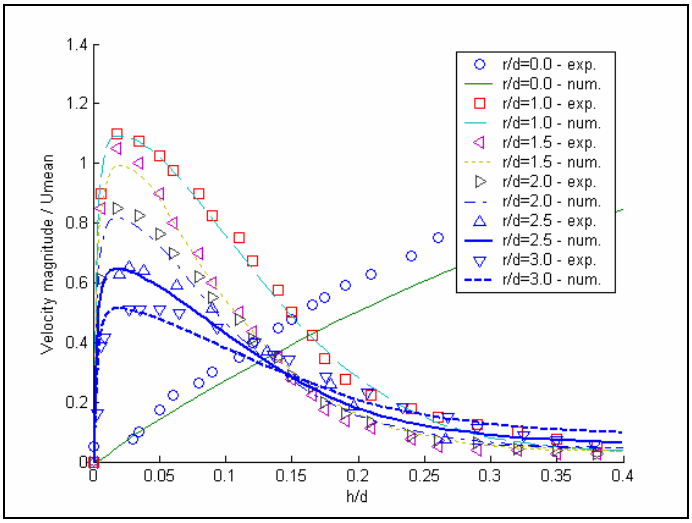

Figure 2. Comparison of FLUENT simulations with experimental data given in [9].

Other authors have also studied experimentally axis-symmetric impinging turbulent jets for a discharge height equal to twice the diameter of the nozzle (i.e., references [10] and [11] in Table 1). In general, most impinging flow jet measurements are carried out along axial directions to provide necessary information for determining the local heat transfer conditions at different radial locations. Fairweather & Hargrave [10] collected both radial and axial flow jet velocity information close to the nozzle discharge region as well as very close to the impinging plate. Some of these measurements correspond to those obtained at a similar location by Geers et al. [11] using a similar fluid at almost the same Reynolds number (see Table 1) but inspecting the flow in the axial direction. Since the two sets of measurements were carried out orthogonally each other, only a few data points can be simultaneously compared with the simulations. Comparisons of the mean velocity components along an axis located at r/D = 0.5 are shown in Figures 3 and 4.

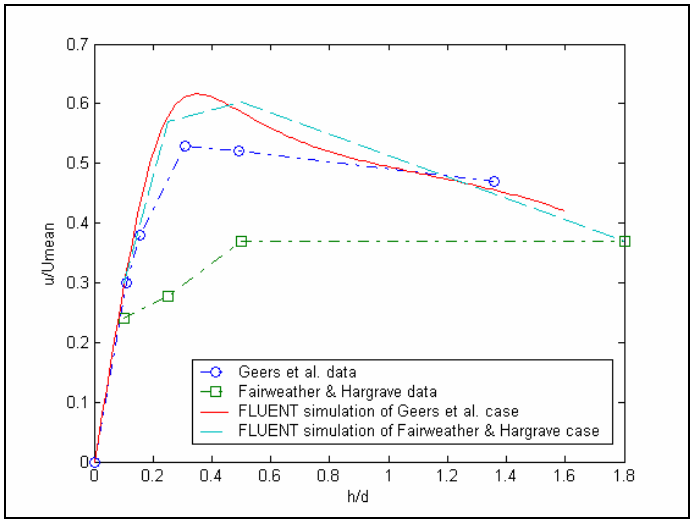

Figure 3. Comparison of simulated axial velocity at *r/D* = 0.5 with data given in [10,11].

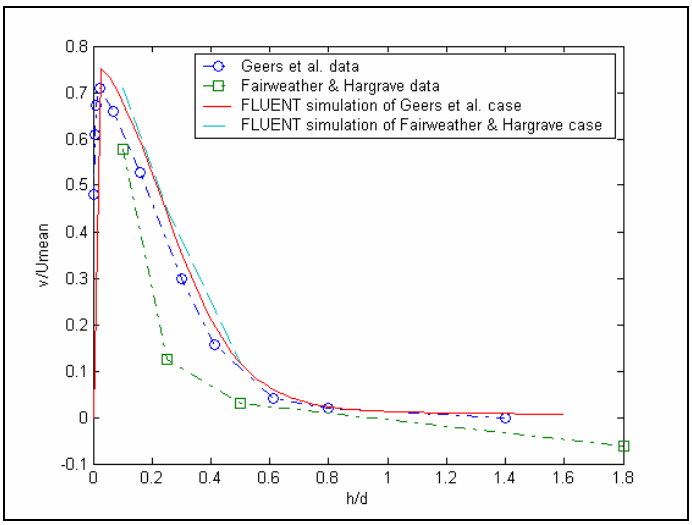

Figure 4. Comparison of the simulated radial velocity at $r/D = 0.5$ with data given in [10, 11].

From these figures, it can be observed that the numerical simulations follow the experimental data of Geers et al. [11] quite well. In turn, the numerical results are not able to follow the experiments carried out by Fairweather & Hargrave [10]. In order to better determine if there is a particular reason that makes the code to fail in simulating the former case, the two data sets are compared with the numerical results for only one axial location. Figures 5 and 6 show these comparisons with data given in [10, 11] at a distance from the nozzle of 1.75D.

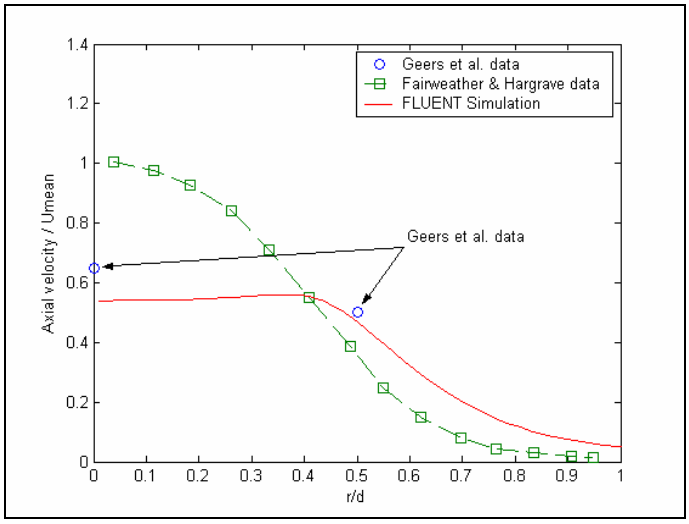

Figure 5. Comparison of simulated axial velocity at $z = 1.75D$ with data given in [10, 11].

Since the Reynolds numbers of both experiments are closer each other, we assume that the data can be compared themselves; thus, it seems that the data given in [10] underestimate the jet spreading. Since the authors have used different experimental techniques and procedures, this affirmation should be taken with precaution. In order to validate our observation, the present simulations are compared also with similar ones carried out by Hadžiabdić & Hanjalić [8] (see Table 1); the results are shown in Figures 7 and 8.

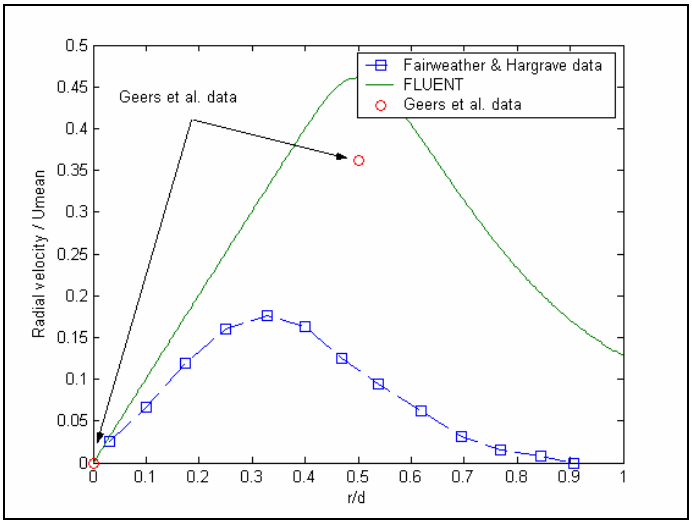

Figure 6. Comparison of simulated radial velocity at $z = 1.75D$ with data given in [10, 11].

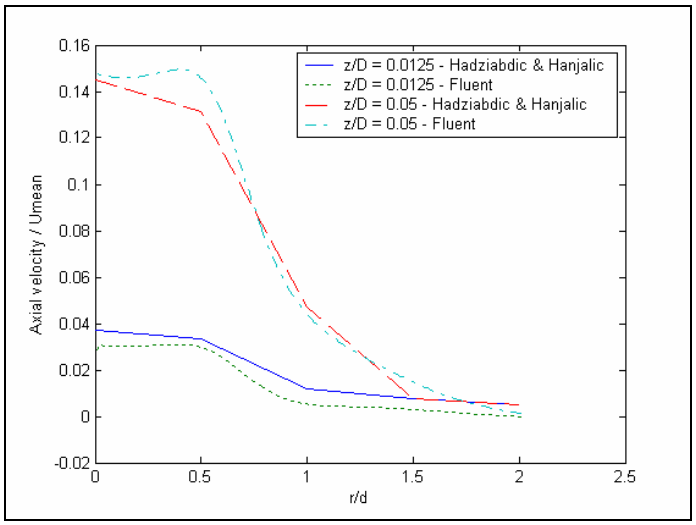

Figure 7. Comparison of present axial velocity calculations with simulations given in [8]

Despite the fact that Hadžiabdić & Hanjalić [8] used the Large Eddy Simulation (LES) approach, while for the present work we use the RANS model available in FLUENT, both simulations, however, are quite similar. Therefore, they confirm the aforementioned observation concerning the data given in reference [10]. Since these data will be used to validate the calculations of the velocity fields in the neighborhood of the impingement, the quality of the data is of prime importance. Moreover, in some cases the velocities were determined by the light dispersion caused by small oil particles injected into the main flow stream [10]. In such a case, inertia effects make it difficult to associate particle velocities to the main flow. In addition, in contact to the plate, the impinging oil particles can be subdivided and dispersed backward creating a cloudy region where the velocity of the transporting fluid becomes very difficult if not impossible to be accurately determined.

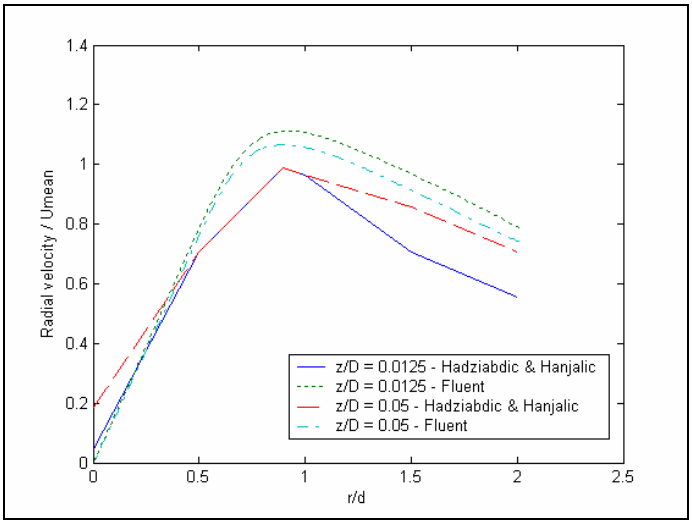

Figure 8. Comparison of present radial velocity calculations with simulations given in [8]

4.2 TURBULENT KINETIC ENERGY IN IMPINGING JETS

A considerable part of impinging turbulent jets studies deals with the heat transfer occurring all along impinging plate. It must be pointed out that the heat transfer can be divided in two principal regions: the impingement area ($r/D < 2$) in which the fluctuating velocity components dominate the heat transfer process, and the wall jet area ($r/D>2$) where the mean fluid motion plays the most significant role for the transport of energy by convection. Thus, modeling turbulence constitutes an important part of turbulent jet studies associated with the understanding of heat transfer and heat transfer enhancement mechanisms. Figure 9 shows the turbulent kinetic energy distribution predicted by FLUENT.

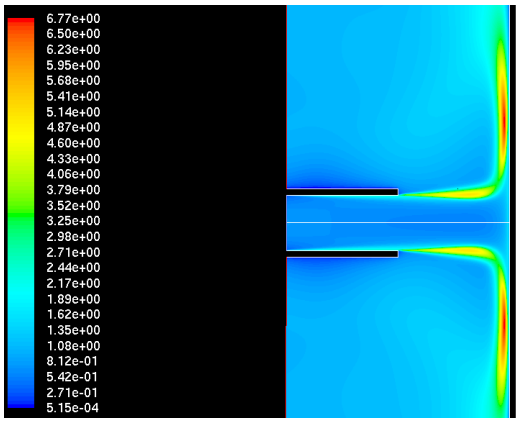

Figure 9. Simulated turbulent kinetic energy distributions.

It is apparent that the turbulent kinetic energy reaches a maximum at two different locations. As expected, the turbulence reaches high values in the shear layer of the jet, before the impingement takes place, in the potential core region. It must be pointed out that several studies were performed at $r/D = 0.5$ to characterize the turbulence intensity along the shear layer (among others: Ashforth-Frost & Jambunathan [13]; Zhang et al. [14]; Isman et al [15]; Geers et al. [11]; Brison & Brun [12]). After the flow is deflected by the solid wall, another maximum occurs in the wall region at a location that extends from $r/D = 1$ to 3.

Geers et al. [11] have shown that the value of the root mean square of the fluctuating velocity components were different according to the direction of the measurements, in both the stagnation and shear layer regions. Thus, the fluctuating velocity fields are strongly anisotropic. Because most of the studies provide the fluctuating velocity components rather than turbulence itself, it is sometimes quite difficult to compare the experimental data with numerical results obtained from κ-ε and κ-ω models, where the transport of turbulence is based on an isotropic turbulence assumption. Instead, it is possible to introduce the mean fluctuating velocity component by using $\kappa = \frac{1}{2}\sum_i u'^2_i$. If $u'_i = u'_j$ for every (*i,j*), then $\sqrt{u'^2_i} = \sqrt{\frac{2}{3}\kappa}$ (i.e., anisotropic turbulence hypothesis). After isolating the r.m.s. value from FLUENT simulations, they are compared with the data of Geers et al. [11]; Figures 10 and 11 show these comparisons.

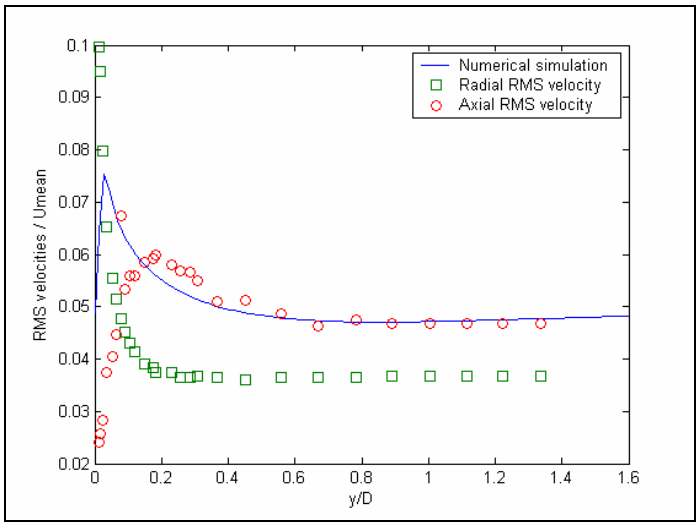

Figure 10. Comparison of fluctuating velocities (simulated) vs. data [11] (*r*/*D* = 0.0).

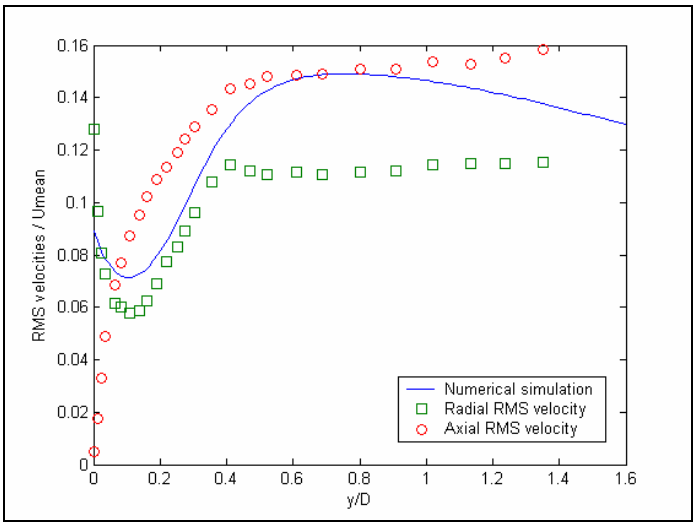

Figure 11. Comparison of fluctuating velocities (simulated) vs. data given [11] (*r*/*D* = 0.5).

From these figures it is observed that the computed turbulent velocities tend to approximate the highest fluctuating component as given by the experiments. In addition, other available experiments were also simulated. To this purpose the experiment cited in Brison & Brun [12] for a Reynolds number equal to 23000, obtained at $r/D = 0.5$ was also simulated. Note that the location of the measurements corresponds exactly to the location where the maximum of the jet shear layer occurs, i.e., where the turbulent fluctuations are the highest in the jet region. All the simulations were carried out using the κ-ε eddy viscosity model. The comparison of the simulations with the data is shown in Figure 12.

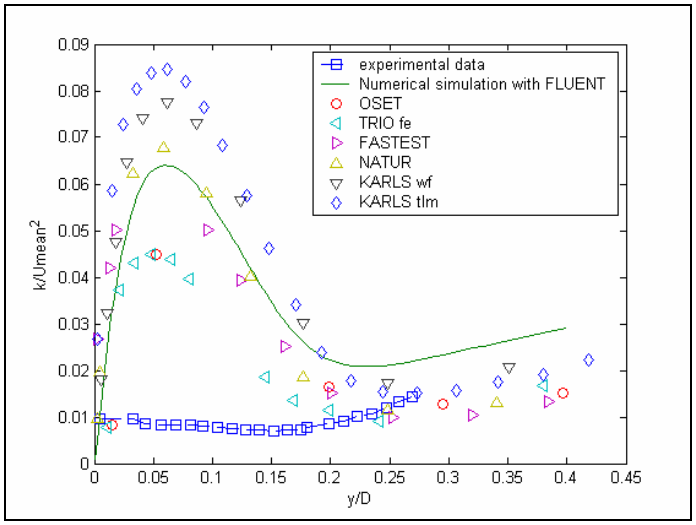

Figure 12. Comparison of simulations using the κ-ε model vs. data given in [12].

Similar to most of CFD codes, FLUENT tends to overestimate the turbulent kinetic energy. It has been pointed out that this excess of turbulent kinetic energy can provoke a 300% overprediction of the heat transfer rate (Ashforth-Frost & Jambunathan [13]). However, beyond a distance of $0.25D$ from the wall, the calculations are in general in good agreement with data. Due to the overprediction observed with the κ-ε model, it seems that it is not appropriated to handle impinging flow. As it was mentioned before, this particular behavior can be due to the fact that this model was initially developed for treating parallel flows. FLUENT provides, however, other optional turbulent models. To study these effects, the simulations were repeated using the following options: κ-ε RNG, κ-ε realizable, κ-ω, κ-ω SST. The results are compared with the five equations RSM model, which takes into account anisotropy effects, in Figure 13. It can be argued that the overprediction associated to the κ-ε model is due to the anisotropy turbulence hypothesis; however, this figure also shows that κ-ε RNG model produces better results than the RSM model. It must be pointed out that a similar observation was given by Zhang et al. [14] who recognized that the overprediction of standard κ-ε and κ-ε RNG models is mainly due to an inappropriate representation of both the turbulent kinetic energy source and dissipation rate terms, rather than the assumption of isotropy. In turn, the Figure 13 also shows that the κ-ω SST model provides results which follow the experimental trends very closely. This model permits the low Reynolds number effects to be taken into account and it is particularly very efficient in the neighborhood of the impingement region. Assuming that this model is the most appropriated for handling impinging flows, the simulations can now be compared with data collected in the regions where the turbulence reaches its maximum. Unfortunately, there is no available experimental data, therefore, the present simu-

lations are compared with similar ones obtained using the LES model by Hadžiabdić & Hanjalić [8]; these comparisons are shown in Figure 14.

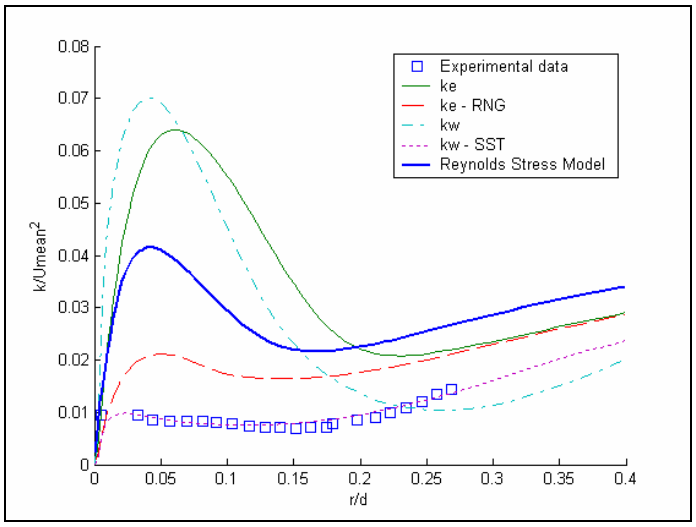

Figure 13. FLUENT simulations carried out with different turbulent models vs. data [12].

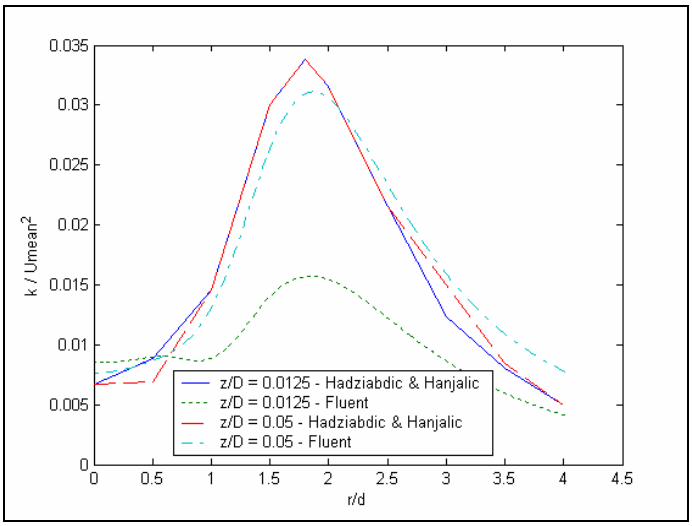

Figure 14. Turbulent kinetic energy distributions obtained using the LES [8] and the κ-ω SST models

At a location z/D = 0.05, the results of both simulations are quite similar and the maximum is reached nearly r/D = 1.8. However, Hadžiabdić & Hanjalić [8] did not observe an influence of the axial position on the distributions. Closer to the wall, i.e., z/D = 0.0125, the normalized distributions obtained with fluent are significantly smaller. This is acceptable because FLUENT imposes a zero turbulent intensity over the wall.

5. CONCLUSIONS

Several turbulence models have been studied; κ – ω SST seems to be the most appropriated for simulating impinging turbulent jets. It permits to correctly represent the turbulence

field in the stagnation region without introducing usually observed overpredictions. All the simulations were in good agreement with the experimental data, except for the Fairweather & Hargrave [10] case. Since FLUENT has been fully validated, numerical experiments can now be performed to simulate discharge length effects. Further, the simulations will provide exhaustive information in such a way that some form of an analytical modeling approach will be developed for calculating the mean velocity fields as well as turbulence in calandria nozzles. The results will help us in achieving a full 3D simulation of the moderator circulation system using moderate computational power.

ACKNOWLEDGMENTS

This work was funded by the Hydro-Québec chair in nuclear engineering and by the NSERC discovery grant # RGPIN 41929.

REFERENCES

[1] Hadaller, G.I., Fortman, R.A., Szymanski, J, Midvidy, W.I. & D.J Train (1996). "Frictional Pressure Drop for Staggered and In-Line Tube Bank with Large Pitch to Diameter Ratio," 17th CNS Conf., Federiction, New Brunswick, Canada.

[2] Huget, R.G., Szymanski, J. & W. Midvidy (1989). "Status of Physical and Numerical Modelling of CANDU Moderator Circulation,"10th Annual Conf. CNS, Ottawa, Canada.

[3] Yoon, C, Rhee, B.W and B.-J. Min (2004) "Development and Validation of the 3-D Computational Fluid Dynamics Model for Candu-6 Moderator Temperature Predictions," Nuclear Technology, Vol. 148, pp. 259-265.

[4] Carlucci, L.N., Agranat, V., Waddington, M., Khartabil, H.F. & J. Zhang (2000). "Predicted and Measured Flow and Temperature Distributions in a Facility for Simulating In-Reactor Moderator Circulation," CFD 2000 Conf., Montréal, Canada.

[5] Yoon, C. & J.H. Park (2006) "CFD Prediction of the Inlet Nozzle Velocity Profiles for the CANDU Moderator Analysis," 27th Annual CNS Conference, Toronto, Canada.

[6] FLUENT User Guide (2005).

[7] Ramezanpour, A., Mirzaee, I., Firth, D. & H. Shirvani (2007) "A Numerical Heat Transfer Study of Slot Jet Impinging on an Inclined Plate," Int. Journal of Numerical Methods for Heat and Fluid Flow, Vol. 17 No. 7, pp. 661-676.

[8] Hadžiabdić, M. & K. Hanjalić (2008) "Vortical Structures and Heat Transfer in a Round Impinging Jet," J. Fluid Mech, Vol. 596, pp. 221-260.

[9] Cooper, D., Jackson, D.C., Launder, B.E. & G.X. Liao (1993) "Impinging Jet Studies for turbulence Model Assessment, Part I: Flow-field Experiments," Int. J. Heat Mass Transfer, Vol. 36, pp 2675-2684.

[10] Fairweather, M. & G.K. Hargrave (2002) "Experimental Investigation of an Axisymmetric, Impinging Turbulent Jet. 1. Velocity Field," Experiments in Fluids, Vol. 33, pp. 464-471.

[11] Leon, F.G., Geers, M., Tummers, J. & K. Hanjalić (2004) "Experimental Investigation of Impinging Jet Arrays," Experiments in Fluids, 36, pp. 946-958.

[12] Brison, J.F. & G. Brun (1991) "Round Normally Impinging Turbulent Jets," 15th Meeting of IAHR Working Group on Refined Flow Modelling, ECL, Lyon, France.

[13] Ashforth-Frost, S. & K. Jambunathan (1996) "Numerical Prediction of Semi-Confined Jet Impingement and Comparison with Experimental Data," Int. Journal for Numerical Methods in Fluids, Vol.23, No. 3, pp. 295-306.

[14] Zhang, Y, Fan J.-Y. & J. Liu (2005) "Numerical Investigation Based on CFD for Air Impingement Heat Transfer in Electronics Cooling," Conference on High Density Micro-system Design and Packaging and Component, Failure Analysis, pp. 1-5.
[15] Isman, M.K., Pulat, E., Etemoglu, A.B. & M. Can (2008) "Numerical Investigation of Turbulent Impinging Jet Cooling of a Constant Heat Flux Surface," Numerical Heat Transfer, Part A, 53, pp. 1109-1132.